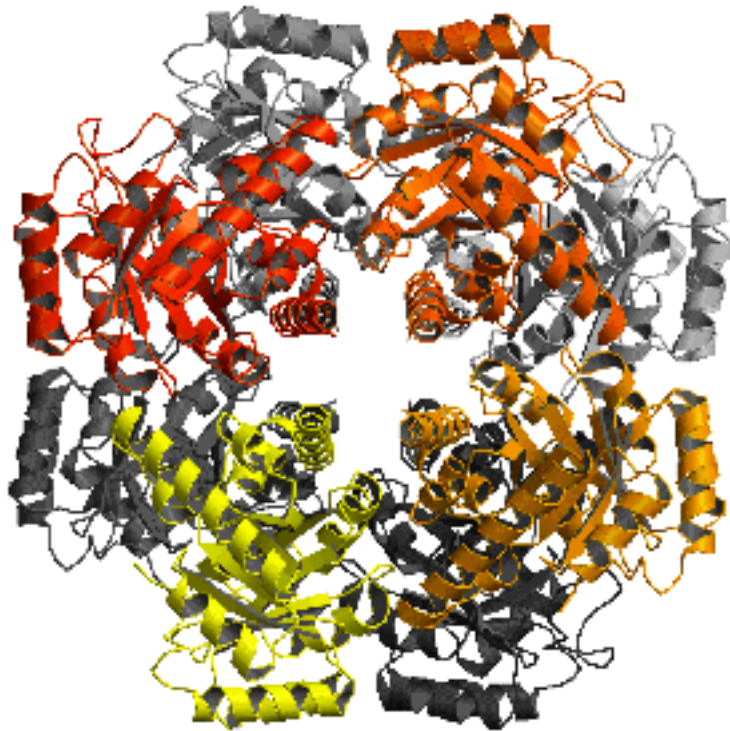**Doctoral Thesis**

# STRUCTURAL AND FUNCTIONAL STUDIES OF PYRIDOXINE 5'-PHOSPHATE SYNTHASE FROM *E. COLI*

**Marta Garrido Franco**

**2002**

# STRUCTURAL AND FUNCTIONAL STUDIES OF

# PYRIDOXINE 5'-PHOSPHATE SYNTHASE FROM *E. COLI*

A dissertation submitted to obtain the degree of

Doctor of Science (Biochemistry and Molecular Biology) presented by

## Marta Garrido Franco

## Max-Planck-Institut für Biochemie

**Abteilung Strukturforschung**

Director of the Thesis

Prof. Dr. Robert Huber

## Universitat Autònoma de Barcelona

**Departament de Bioquímica i Biologia Molecular**

Tutor of the Thesis

Prof. Dr. Francesc X. Avilés

## 2002

A mis padres Antonio Miguel y Ana María,

A mis hermanos Eduardo y Clara.

A Tim.

"Far away there in the sunshine

are my highest aspirations.

I may not reach them, but

I can look up and see their beauty,

believe in them, and try to follow

where they lead."


Louisa May Alcott

Part of the work presented here has been previously published in:

1. **Garrido-Franco, M.**, Huber, R., Schmidt, F.S., Laber, B. and Clausen, T. (2000). Crystallization and preliminary x-ray crystallographic analysis of PdxJ, the pyridoxine 5'-phosphate synthesizing enzyme. *Acta Cryst. Sect. D* **56**:1045-1048.

2. **Garrido-Franco, M.**, Laber, B., Huber, R. and Clausen, T. (2001). Structural basis for the function of pyridoxine 5'-phosphate synthase. *Structure* **9**:245-253.

3. **Garrido-Franco, M.**, Laber, B., Huber, R. and Clausen, T. (2002). Enzyme-ligand complexes of pyridoxine 5'-phosphate synthase: implications for substrate binding and catalysis. *J. Mol. Biol.* (Submitted)

**TABLE OF CONTENTS**

**SUMARIO**

El piridoxal 5'-fosfato es la forma biocatalíticamente activa de la vitamina $B_6$, siendo uno de los cofactores más versátiles de la naturaleza, el cuál tiene un papel central en el metabolismo de aminoácidos. Mientras que la mayoria de microorganismos y plantas pueden sintetizar la vitamina $B_6$ *de novo*, los mamíferos se ven obligados a obtener uno de sus vitámeros a través de la dieta. La maquinaria biosintética de *Escherichia coli* es, de lejos, la mejor caracterizada y consiste en cuatro proteínas pdx. PdxJ, también conocida como piridoxina 5'-fosfato sintasa, es la enzima clave en esta via. Cataliza el último paso, la complicada reacción de cierre del anillo entre 1-deoxi-D-xilulosa-5-fosfato y aminoacetona-3-fosfato para formar piridoxina 5'-fosfato. La comparación de secuencias de PdxJ entre espécies revela que existe un alto grado de conservación indicando así la enorme importancia fisiológica de esta enzima.

Con el uso de un derivado de mercurio fue posible el resolver la estructura cristalina de la enzima de *E. coli* por el método del "single isomorphous replacement with anomalous scattering" y el refinar la estructura a 2.0 Å de resolución. El monómero corresponde al plegamiento TIM o barril (_/_)$_8$, con la incorporación de tres hélices extra que median los contactos entre intersubunidades en el octámero. El octámero representa el estado fisiológicamente relevante, que fué observado tanto en el cristal como en solución, y que esta organizado como un tetrámero de dímeros activos. La caracterización de la estructura cristalográfica de la enzima con sustratos, análogos de sustrato y productos unidos permitió la identificación del centro activo y la propuesta de un mecanismo detallado. Los rasgos catalíticos más remarcables son: (1) el cierre del centro

activo una vez se han unido los sustratos, de manera que el bolsillo de unión queda aislado del solvente y los intermediarios de la reacción quedan así estabilizados; (2) la existencia de dos sitios de unión de fosfato bien definidos; (3) y un canal de agua que penetra el núcleo del barril _ y permite liberar las moléculas de agua formadas durante la reacción.

La cantidad de información presentada debería permitir el diseño de inhibidores de la piridoxina 5'-fosfato sintasa basados en su estructura. Es interesante el destacar que entre las bacterias que contienen el gen *pdxJ* se encuentran unos cuantos patógenos bien conocidos. La resistencia de bacterias contra antibióticos está aumentando cada vez más, hecho que se está convirtiendo en un auténtico problema. Por este motivo, es necesario el desarrollar medicamentos antibacterianos con un alto grado de especificidad y la piridoxina 5'-fosfato sintasa parece ser una diana muy prometedora.

**SUMMARY**

Pyridoxal 5'-phosphate is the biocatalytically active form of vitamin $B_6$, being one of nature's most versatile cofactors that plays a central role in the metabolism of amino acids. Whereas microorganisms and plants can synthetise vitamin $B_6$ *de novo*, mammals have to obtain one of the $B_6$ vitamers with their diet. The *Escherichia coli* biosynthetic machinery is the, by far, best characterised and it consists in four pdx proteins. PdxJ, also referred to as pyridoxine 5'-phosphate synthase, is the key enzyme in this pathway. It catalyses the last step, the complicated ring-closure reaction between 1-deoxy-D-xylulose-5-phosphate and aminoacetone-3-phosphate yielding pyridoxine 5'-phosphate. Sequence comparison of PdxJ from different species revealed a remarkable high degree of conservation indicating the paramount physiological importance of this enzyme.

With the use of one mercury heavy-atom derivative, it was possible to solve the crystal structure of the *E. coli* enzyme by the single isomorphous replacement method with anomalous scattering and to refine the structure at 2.0 Å resolution. The monomer folds as a TIM or $(\_/\_)_8$ barrel, with the incorporation of three extra helices that mediate intersubunits contacts within the octamer. The octamer represents the physiological relevant state that was observed in the crystal and in solution, and that is organised as a tetramer of active dimers. Characterisation of the enzyme crystal structure with bound substrates, substrate analogues, and products allowed the identification of the active site and the proposal of a detailed reaction mechanism. The most important catalytic features are: (1) active site closure upon substrate binding, in order to isolate the specificity pocket from the solvent und thus stabilise the reaction intermediates; (2) the existence of two

well-defined phosphate binding sites; (3) and a water channel that penetrates the _ barrel core and allows the release of waters in the closed state.

The amount of information here presented should permit the structure-based design of pyridoxine 5'-phosphate synthase inhibitors. Interestingly, among bacteria that contain the *pdxJ* gene there are several well-known pathogens. More and more, the bacterial resistance against antibiotics is increasing and therefore becoming a real problem. Thus, it is necessary the development of highly specific antibacterial drugs and pyridoxine 5'-phosphate synthase seems to be a promising novel target.
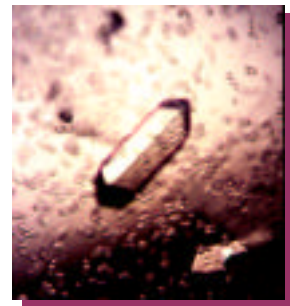
# 1. INTRODUCTION

## 1.1. THE BIOCHEMISTRY OF PYRIDOXAL 5'-PHOSPHATE

### 1.1.1. Pyridoxal 5'-phosphate biosynthesis

The biocatalytically active form of vitamin $B_6$ (pyridoxine, pyridoxol), pyridoxal 5'-phosphate (PLP) is of paramount physiological importance due to its enormous catalytic versatility as the central coenzyme in amino acid metabolism. Besides PLP, pyridoxamine 5'-phosphate (PMP) plays an important role in the biosynthesis of deoxysugars. In contrast to mammals, which derive vitamins exclusively from their diet, prokaryotes can synthesise vitamin $B_6$ *de novo*. Therefore, inhibition of vitamin $B_6$ biosynthesis represents a novel therapeutic strategy and the participating enzymes are promising targets for the development of new antibacterial agents.

Studies on the biosynthesis of vitamin $B_6$ have been focused on *E. coli*, in which the five genes for *de novo* synthesis of pyridoxine have been identified via complementation of pyridoxine auxotrophic mutants and tracing experiments using radioactive labelled precursors (Drewke *et al.*, 1996; Hill and Spenser, 1996; Hockney and Scott, 1979; Lam and Winkler, 1990; Lam and Winkler, 1992; Roa *et al.*, 1989; Schoenlein *et al.*, 1989; Yang *et al.*, 1998; Zhao and Winkler, 1996). While two of the defined genes (*serC* and *gapB*) are also involved in other biosynthetic pathways, the gene products of *pdxA*, *pdxB* and *pdxJ* are unique to pyridoxine biosynthesis. GapB, SerC and PdxB are involved in the synthesis of the non-proteinogenic amino acid 4-(phosphohydroxy)-L-threonine (4PHT), one of the two acyclic vitamin $B_6$ building blocks. PdxA and PdxJ are required for the condensation of HTP with the second building block, 1-deoxy-D-xylulose-5-

phosphate (DXP), to yield pyridoxine 5'-phosphate (PNP). The different $B_6$ vitamers pyridoxine (PN), pyridoxal (PL), pyridoxamine (PM), PLP, and PMP are generated from PNP and interconverted into each other in the so-called salvage pathway by the action of the ATP-dependent kinase PdxK, various transaminases and the FMN-dependent oxidase PdxH (Dempsey, 1987; Hill and Spenser, 1986; Tryfiates, 1986; Yang *et al.*, 1996). This salvage pathway is ubiquitously distributed.

The exact roles of PdxA and PdxJ, however, remained undetermined for a long time. Only recently, it was demonstrated that PdxA is an NAD-dependent dehydrogenase that catalyses the oxidative decarboxylation of HTP to give the unstable intermediate aminoacetone 3-phosphate (AAP) (Cane *et al.*, 1998). PdxJ then catalyses the consecutive reaction in which AAP and DXP are condensed to yield PNP and inorganic phosphate ($P_i$) (Cane *et al.*, 1999; Cane *et al.*, 2000; Laber *et al.*, 1999), and has therefore been named PNP synthase (Fig. 1).

Recent findings suggest that vitamin $B_6$ functions besides its vital coenzyme role as an antioxidant that quenches singulet molecular oxygen during photooxidative stress (Bilski *et al.*, 1999; Ehrenshaft *et al.*, 1998). The gene *SOR1* (singulet oxygen resistance, also called *pdx1*, *pyroA*) was identified in *Cercospora nicotianae* and *Aspergillus nidulans* as the responsible element for this resistance (Ehrenshaft *et al.*, 1999; Osmani *et al.*, 1999). As it was demonstrated in further experiments, the SOR1 protein is specifically required for PNP biosynthesis although no homology to any of the well-known *E. coli pdx* genes exists. The outstanding physiological importance of SOR1 is expressed by its remarkable high degree of conservation in nature (Ehrenshaft *et al.*, 1998). Sequence database analysis indicated that organisms encode either SOR1 or the *E. coli* vitamin $B_6$

biosynthetic genes *pdxA*/*pdxJ*. The SOR1 group includes fungi, plants, archaebacteria and

some eubacteria whereas the *pdxA*/*pdxJ* group comprises only eubacteria. Therefore,

Ehrenshaft and coworkers postulated that the two divergent pathways for *de novo* vitamin

$B_6$ biosynthesis developed early during evolution of the eubacteria (Ehrenshaft *et al*.,

1998).
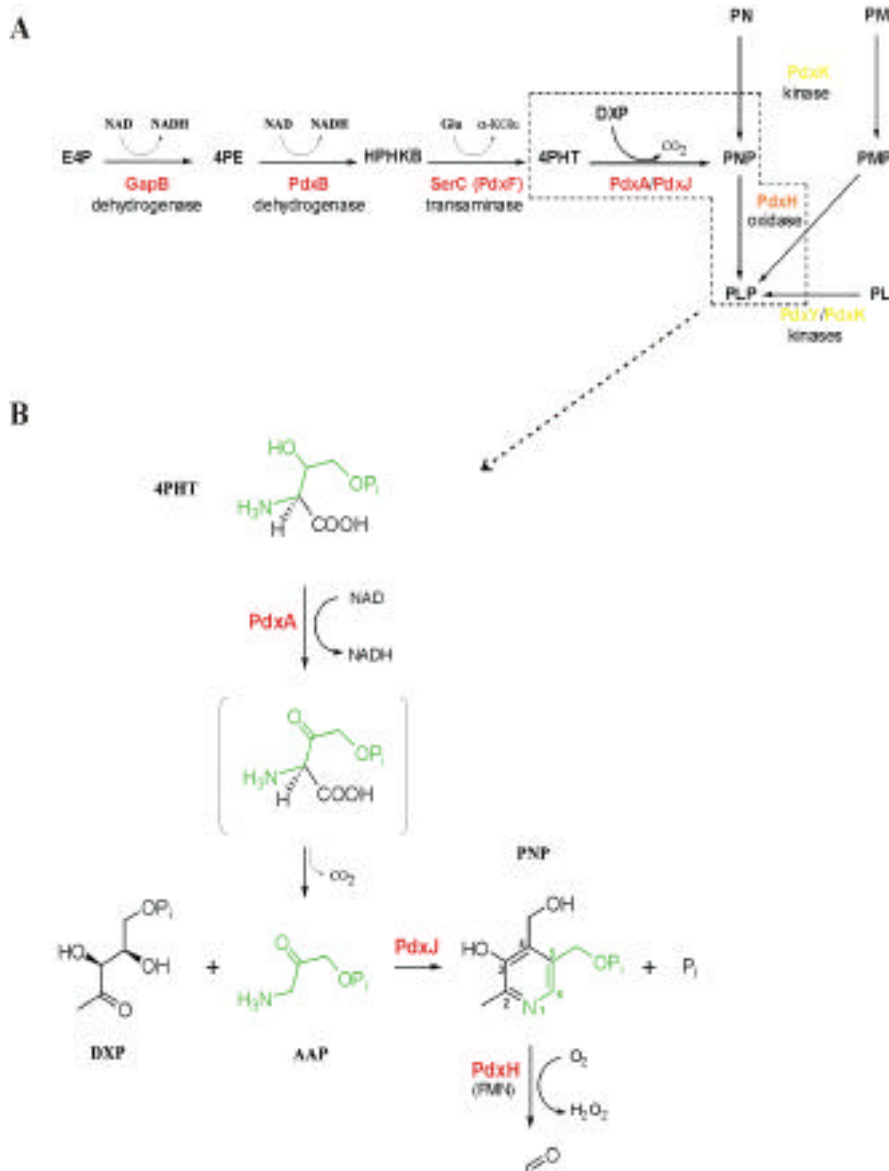


**FIGURE 1.** Detailed scheme about PLP formation. **A)** Interconnection between the *de novo* and the salvage pathways. In red are coloured the *de novo* enzymes and in yellow are the "salvage" enzymes. PdxH, that takes part in both pathways, is coloured orange. The abbreviations are as follows: E4P, erythrose 4'-phosphate; 4PE, 4-phosphoerythronate; HPHKB, 3-hydroxy-4-phosphohydroxy- -ketobutyrate; 4PHT, 4-phosphohydroxy-L-threonine; DXP, 1-deoxy-D-xylulose-5-phosphate; PN, pyridoxine; PNP, pyridoxine 5'-phosphate; PM, pyridoxamine; PMP, pyridoxamine 5'-phosphate; PL, pyridoxal; PLP, pyridoxal 5'-phosphate. **B)** Formation of PNP and PLP in the recently established *de novo* pathway. In the presence of PdxA, NAD, 4HTP and DXP, PdxJ catalyses the ring closure to yield PNP and inorganic phosphate. Afterwards, PdxH oxidize PNP to PLP.

## 1.1.2. Pyridoxal 5'-phosphate, a versatile enzymatic cofactor

Vitamin $B_6$, in the form of its biocatalytically active phosphorylated derivatives PLP and PMP, represents one of nature's most flexible cofactors. PLP dependent enzymes play a major role in the metabolism of amino acids, showing a remarkable catalytic versatility: PLP enzymes catalyse a wider spectrum of chemical transformations than any other cofactor dependent enzyme.

In 1974 Dunathan and Voet proposed an evolutionary hypothesis (Dunathan and Voet, 1974) about the possibility of a common ancestor for all PLP-dependent enzymes. This hypothesis was based on the fact that all PLP enzymes, analysed by Dunathan, were following a similar reaction mechanism, in which proton addition to the C-4' of the coenzyme occurred with the same stereochemistry. Accordingly, it was deduced that all these enzymes have bound the coenzyme in the same orientation, with its *re* face (respective to the aldimine linkage) towards the protein (Fig. 2). The evolutionary hypothesis proposes that the reaction specificity occurred first and that only afterwards the substrate specificity played a relevant role. The mechanistic explanation can be that several structural changes and adaptations are undergone to achieve perfection in catalysis, an adjustment that appear be more important than adaptation for substrate binding. Metabolically, a preference appears to exist to accelerate the reaction with several substrates rather than to catalyse the transformation of a single substrate.

All PLP enzymes, without exception, carry the cofactor covalently bound as an imine to the -$NH_2$ group of an active site lysine, a state known as the "internal" aldimine. After formation of the Michaelis complex, in which the substrate is non covalently fixed in the

active site of the enzyme, the amino group of the PLP-binding lysine is displaced by the

amino group of the substrate amino group yielding the "external" aldimine. This so-called

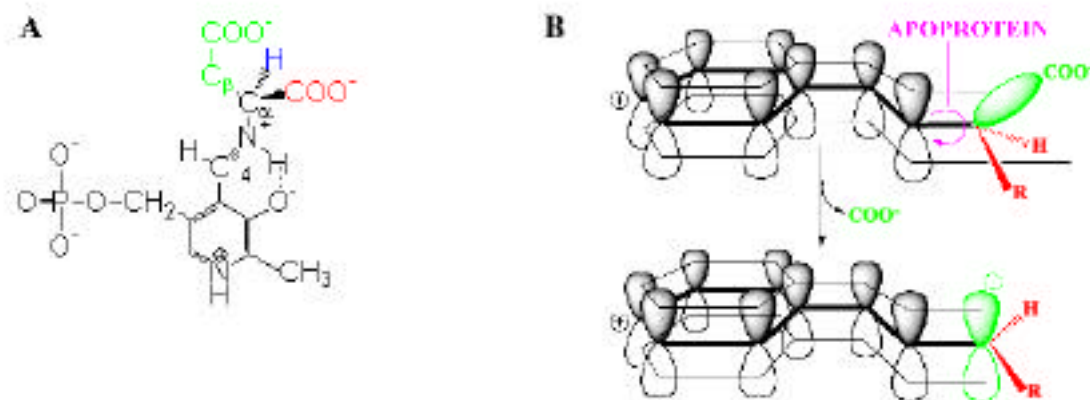transaldimination is the starting step of PLP-catalysed reactions (Fig. 3,4).

**FIGURE 2.** The pyridoxal 5'-phosphate cofactor. **A)** *Si* face view; the C  substituents are distinctly coloured. **B)** Stereo representation of the C  substituents. In this example the carboxyl group will be eliminated in the following steps during the reaction. Shown are the  -orbitals of the pyridine ring.

Due to its "electron sink" character, mainly achieved by the electrophilic positively

charged nitrogen of the pyridine ring, the PLP withdraws electrons from the substrate in

the external aldimine. The developing negative charge resulting from, e.g., C -proton

abstraction can be delocalised and therefore stabilised in the  -electron system of the

pyridine in the Schiff base form. The type of the reaction is determined by the orientation

of the C  substituents: the C  bond of the substrate that is perpendicularly oriented to the

PLP-imine  system plane will cleave (Fig. 2B). Depending on the eliminated group, e.g.

$H^+$, $CO_2$ or R, different reaction types arise like transamination, racemisation,  -

decarboxylation, aldol cleavage,  − or  −elimination or  − or  − replacement. The

release of any of the three C  substituents results in a resonance stabilised carbanion, the

so-called quinonoid, which is the central intermediate of the proposed PLP dependent

reaction mechanisms. The numerous distinct reactions that are catalysed by this superfamily of enzymes are illustrated in Figure 4.
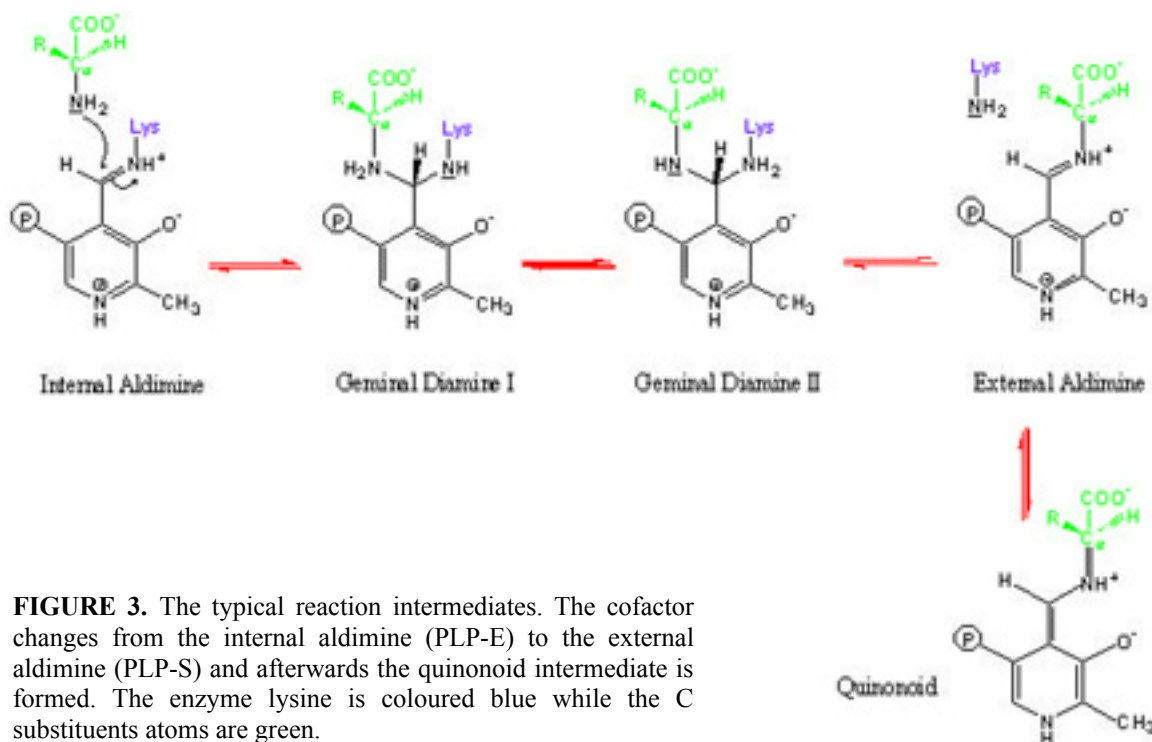


**FIGURE 3.** The typical reaction intermediates. The cofactor changes from the internal aldimine (PLP-E) to the external aldimine (PLP-S) and afterwards the quinonoid intermediate is formed. The enzyme lysine is coloured blue while the C substituents atoms are green.

In all three-dimensional structures solved so far, the imine nitrogen is hydrogen-bonded to O3'. This interaction guarantees the coplanarity between the imine double bond and the pyridine ring (Fig. 2A). The phosphate group situated at C-5 provides a firm anchor to the coenzyme that is usually bound by the positive end of an  -helix, and by several hydrogen bonds and salt bridges with specific protein residues. The C-2 methyl group is considered as functionless being an appendix during evolution. This group is usually bound in a hydrophobic pocket of the protein.
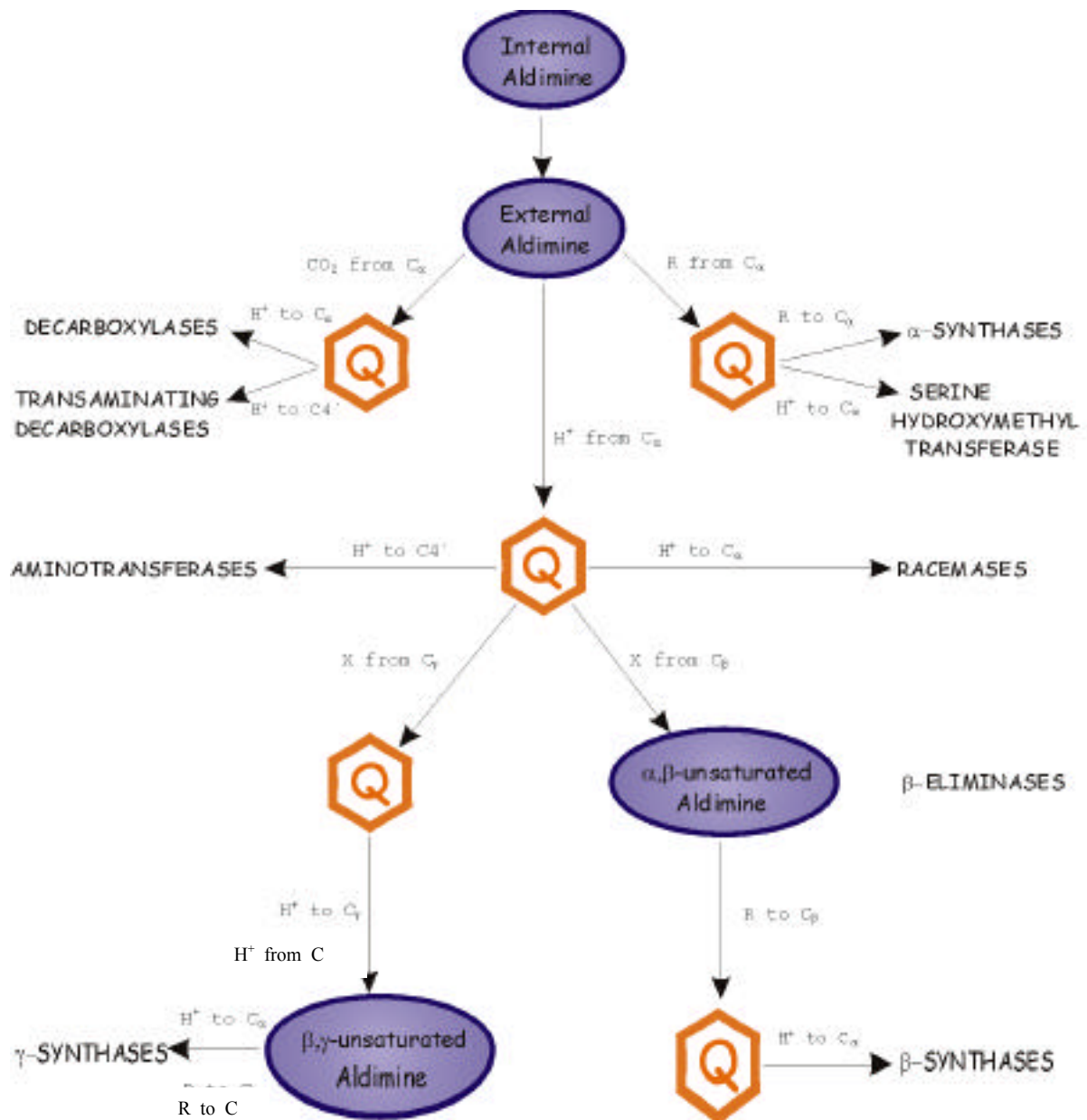
**FIGURE 4.** Overview of the diverse reactions catalysed by PLP-dependent enzymes. The quinonoid intermediate is represented in orange. This is an adapted version of the R. A. John figure (John, 1995).

Another important physical property of the $B_6$ vitamers are their characteristic absorption spectra. Due to the delocalised electron system on the pyridine ring (John, 1998). The PLP chromophor absorbs in the region from $340 - 550$ nm. Since different PLP derivatives exhibit different absorption bands, spectroscopic analysis is a powerful

instrument to follow the state of the cofactor during the reaction (Fig. 5). When the imine nitrogen of the internal and external aldimine is protonated, electron delocalisation is extended yielding the most prominent absorption peak, with a $_{max}$ value around 420 nm (**I**). This chromophor is also the reason for the typical yellow colour of PLP-dependent enzymes. Around 340 nm (**II**), the ketimine is the most probable intermediate. Due to the sp3 hybridation of the pyridine C4, –electron delocalisation is reduced resulting in a chromophor absorbing at start wavelengths. During a PLP-catalysed reaction, most often a quinonoid intermediate is formed, which has a characteristic long-wavelength maximum at approximately 490 nm (**III**). The shift to longer wavelength is caused by the –delocalisation. Nevertheless, spectra analysis is quite complicated in practice. Even if there is a clear separation in the peak maximums, each specie contributes to the complete spectra thereby impeding to resolve the individual spectra.
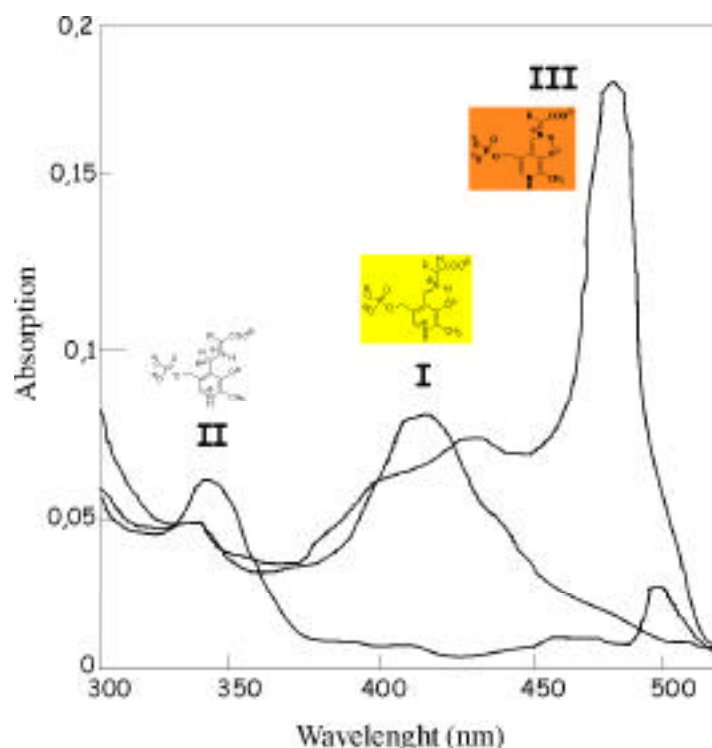


**FIGURE 5.** Example of different absorption spectra recorded in a stopped-flow measurement. Absorption scans at different times reveal the successive intermediates of the reaction. These intermediates can be identified by correlating the absorption peak with theoretical values.

## 1.2. FUNDAMENTALS OF PROTEIN CRYSTALLOGRAPHY

### 1.2.1. Crystallisation of proteins

'Crystal' derives from the Greek word 'krustalos', which means 'clear ice', because quartz was the archetype. The aim for each crystallographer is to obtain suitable sized crystals, a task that can be the limiting step to solve protein three-dimensional structures by X-ray diffraction methods. Under certain circumstances proteins arrange themselves to form crystals. Each of the single biological molecules adopt one or few orientations resulting in an orderly three-dimensional array stabilised by non-covalent interactions such as salt bridges, hydrogen bonds, van der Waals or dipole-dipole interactions. The success to achieve precipitation and further ordering depends on so many parameters that the variation of many of them in a trial-and-error manner is the only procedure to establish the optimal precipitant conditions. Parameters such as temperature, pH, ionic strength, concentration of protein and organic solvent, or ratio of the protein solution *versus* the precipitant solution need to be screened.

Indispensable for crystallisation is to bring the protein to a supersaturated state (Fig. 6). The Debye-Hückel theory describes how the solubility of a protein depends on the present ions. At low ionic strength (low ionic concentration), the solubility of a protein is higher if the amount of electrolites is increased: "salting in". At high ionic strength the ions start to compete with each other about water molecules, resulting in a decrease in solubility. This happening is known as "salting out". The crystallographer can shift the equilibrium from solution to supersaturation by increasing or reducing the ionic strength

of the protein solution. The Hofmeister series indicate that at high ion concentration small ions with a high charge are generally most effective. For proteins, much larger and with complicated surface charge distributions, this theory is not sufficient to explain the phenomenon of crystal formation. For instance, the difference between the free energies ($\Delta$ G) of the solid and soluble states will indicate the favourable trend. In general, the electrostatic interactions in crystals are much more favourable than the "interactions" in amorphous precipitates. The main parameters than influence protein solubility are temperature, pH or presence of precipitants or organic solvent. At high ionic strength most proteins are more soluble at low temperatures, a statement that is inverted at low ionic strength. Normally, a highly charged protein is more soluble. This situation can be changed by altering the pH because protons are added or abstracted, resulting in a net change of the charge. The isoelectric point is the pH of a protein, when its charge is 0. In this special case the solubility of the protein is minimal. Organic solvents, added to an aqueous solution, decrease its dielectric constant thereby decreasing the solubility due to the reduced coulombic attractions. Solvents as ethanol, acetone, acetonitrile or 2-methyl-2,4-pentanediol (MPD) are commonly used to precipitate proteins. However, organic solvents often results in the denaturation of the protein.

As shown in Figure 6, crystal growth can be divided into two steps. First, a spontaneous nucleus formation occurs in the supersaturation area followed by formation of small aggregates. After the critical amount of aggregated molecules (10-200) is surpassed, the crystal growth is an energetically favoured process. Crystal growth always needs a lower degree of supersaturation than nucleus formation. Crystals should grow slowly enough to achieve the possible maximum internal order.
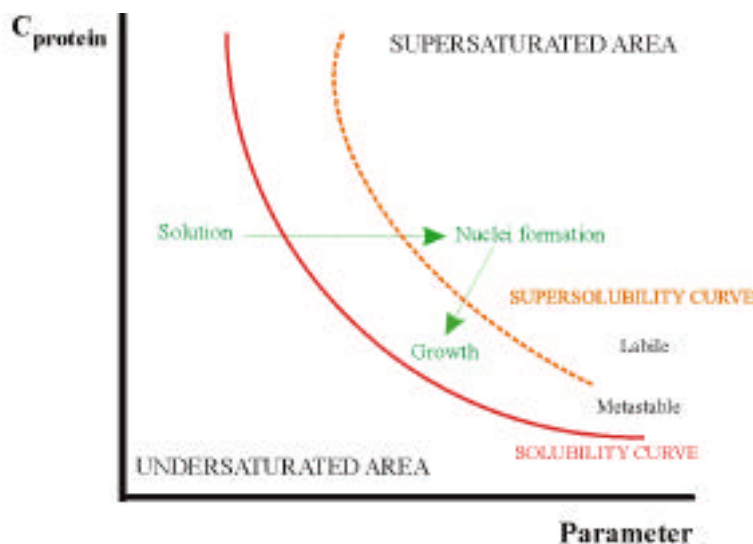
**FIGURE 6.** Solubility diagram. It includes where the different steps occurring during crystal formation take place (highlighted in green). The supersolubility curve limits the labile region, where nucleation happens, from the metastable region, where crystals grow.

It is clear that crystal morphology is not a direct synonym of crystal quality. "Good-looking" crystals can have disordered crystal packing limiting their diffraction properties. Contrary, some "awful" crystals can give a positive surprise while measuring them.

Different methods for growing protein crystals, as batch crystallisation, dialysis, liquid-liquid diffusion and vapour diffusion, have been established and developed in the direction of using less amounts of material. For a very long time, crystallisation attempts needed some hundred milligrams of protein for growing crystals and around one gram of protein to finish X-ray structure solution. With development of microtechniques, smaller amounts are needed. If we consider that a crystal, with typical dimensions 0.3 x 0.3 x 0.3 mm, is formed by around 15 µg, 1 mg of protein would be needed to grow more or less 65 crystals.

The general rule, while trying to crystallise a protein, is that the protein sample must be pure and homogeneous. In other words, it must be cleaned from small undesirable molecules and contain a population with the same protein conformation.

Microheterogeneity of the sample can occur because of different sources: variation in primary structure (genetic mutations), secondary structure (unfolding), tertiary structure (conformers), quaternary structure (oligomerisation), as a partial oxidation of some groups as sulfhydryl in proteins, fragmentation by proteolysis or molecular dynamics on flexible parts. As crystals will be used for data collection, it is important that they have the best possible quality in order to obtain a suitable structural data. For this reason, twinned crystals (crystals growing into each other at different orientations) or with an inadequate size have to be improved. When different crystal forms are obtained the best diffracting crystals with the highest symmetry should be chosen for further work.

### 1.2.1.1. The seeding technique

Seeding has often been used as a method of last resort or in situations when, after successful crystallisation, no further crystals or no crystals with the same quality and size could be reproduced. Equal which method was used to obtain the initial crystals, seeding may be a good choice to optimise the rate of growth and the size of the crystals with a high degree of reproducibility. When crystals seeds are added to an equilibrated protein solution, the first step of crystallisation, i.e. nuclei formation, is circumvented. In the case of spontaneous nucleation, a new seed must be generated while competing with other events, e.g., aggregation. Seeding may provide a method to overcome difficulties like initial growth after nucleation achieved too fast, which results in incorporation of defects, or disorder in the spontaneous formed nuclei. Therefore, the seeds to be further used have to be selected from the best initial crystals.

Seeding can be homogeneous or heterogeneous. By homogeneous seeding we understand that the crystals to be used and the fresh protein solution to be seeded are from the same source. In this kind of seeding we can differentiate micro from macroseeding. In microseeding, microcrystals are transferred to a pre-equilibrated fresh protein drop. In macroseeding, crystals are enlarged by introducing pre-grown (washed) crystals in a fresh solution. In the heterogeneous seeding either the seeds originated from a different protein (respective to the one to be crystallised) or a regular surface, e.g., a nitrocellulose fibre, is introduced to the drop providing the "regular lattice" for nucleation.

In practice, the following steps have to be done:

1. Determination of the optimal conditions for seeding. For example the time for pre-equilibration of the fresh protein drop or crystallisation setup has to be optimised, the different methods like sitting-drop or hanging-drop vapour-diffusion methods have to be checked.

2. Preparation of the probe by mounting an animal whiskers (normally rabbit) with wax to the end of a thick-walled capillary.

3. The end of the whisker is used to touch an existing crystal (Fig. 7). Then, some of the crystal seeds will remain attached and could be introduced into a pre-equilibrated drop by running it in a straight line across. The growth of crystals along the drawn line indicates that the condition might be suitable for seeding techniques. It can also occur that self-nucleated crystals appear away from the streak line.

4. The optimisation of the seeding steps is intended to grow single well-ordered crystals of suitable size that do not grow into each other.
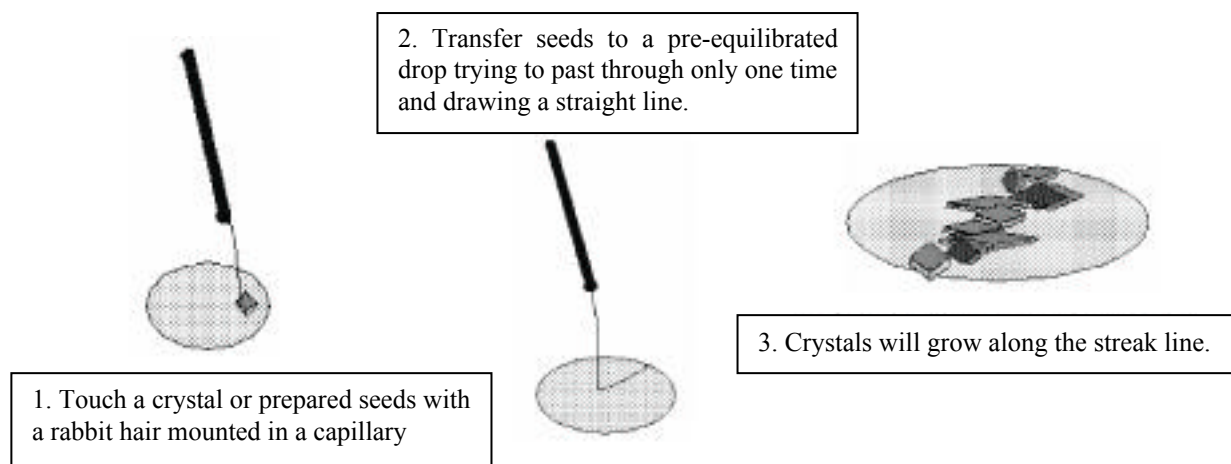
2. Transfer seeds to a pre-equilibrated drop trying to past through only one time and drawing a straight line.

3. Crystals will grow along the streak line.

1. Touch a crystal or prepared seeds with a rabbit hair mounted in a capillary

**FIGURE 7.** The seeding technique. Crystal can be grown if one or more crystal seeds are transferred to a fresh drop consisting of protein and precipitant solution. In this way, the limiting nucleation step is already achieved and therefore, the growing of good sized crystals should be theoretically faster.

**1.2.1.2.** Crystal symmetry and space groups

Crystals exhibit clear cut faces and edges that are related to the periodic arrangement of the contained molecules. The unit cell is defined as the minimal structural piece that repeats in all three dimensions to build up the crystal. Almost all crystals contain symmetry elements, with the exception of triclinic crystals, which is reflected by the fact that the unit cell will contain more than one object. The so-called asymmetric unit is the basic repeating object that is related to all other identical objects in the unit cell by the symmetry elements. Because proteins are enantiomorphic (only L- and not D-amino acids are relevant), neither mirror planes nor inversion centres are observed in protein crystals. As a consequence, the 230 possible space groups are reduced to 65, and distributed between 7 crystal systems: triclinic, monoclinic, orthorhombic, tetragonal, trigonal, hexagonal and cubic. The combination of the 4 crystal lattices, primitive (P), body centred (I, from the German Innenzentrierte), face centred (F) or centred in the (010) planes (C) with the 7 crystal systems allows a total of 14 Bravais lattices.

### 1.2.2. X-ray diffraction by crystals

The diffraction or scattering of X-rays is based on the interference phenomena. X-rays are electromagnetic waves that interact with the electrons and as a consequence, the electrons oscillate with the same frequency as the incident wave acting as radiation scatters. In crystallography, X-rays are used to "visualize" atoms in a macromolecular structure, since the radiation has to be in the same range as the object of interest, the interatomic distances are 0.15 nm = 1.5 Å. In the electromagnetic spectrum, this wavelength corresponds to the X-ray region.

Braggs law (Bragg and Bragg, 1913) interprets X-ray diffraction by a crystal lattice as a conjunct of reflections from different planes of atoms in the crystal (Fig. 8). For a constructive interference, this can be written as follows:

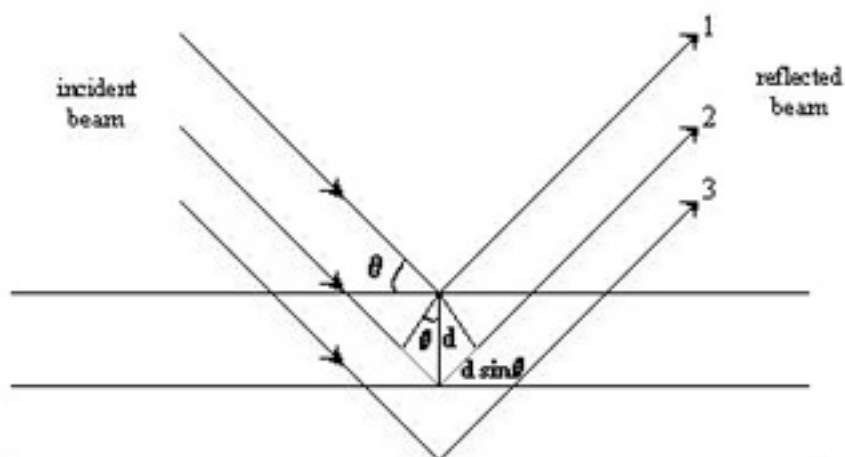$$2d \sin \theta = n\lambda \qquad \qquad \textbf{(equation 1)}$$



**FIGURE 8.** Scheme that explains Bragg's law. Two waves that are reflected by two adjacent lattice planes with distance **d** have a difference in path length that is equal to $2d\sin\theta$, shown in red. A prerequisite for constructive interference is that this difference in path is an intenger multiple **n** of the wavelength λ used.

where d is the separation between successive planes of atoms, is the angle of incidence

of the X-rays that equals the angle of reflection, n is an integer and is the wavelength of

the X-rays (usually corresponding to the Cu K radiation = 1.5418 Å). When n = 1, then d

= $d_{min}$ and = $_{min}$. This condition is equivalent to the highest resolution for the crystal

diffraction.

The Ewald construction allows the geometrical interpretation of Bragg's law (Ewald,

1921). With the crystal at its centre (C), a sphere is drawn of radius 1/ . The origin (O) of

the reciprocal lattice is taken as the point where the X-ray beam leaves the sphere after

passing through the crystal (Fig. 9). Thus, collection of a complete data set will be

possible only if the crystal (and detector) is moved in such a way that every reciprocal

lattice point passes through the sphere of reflection.



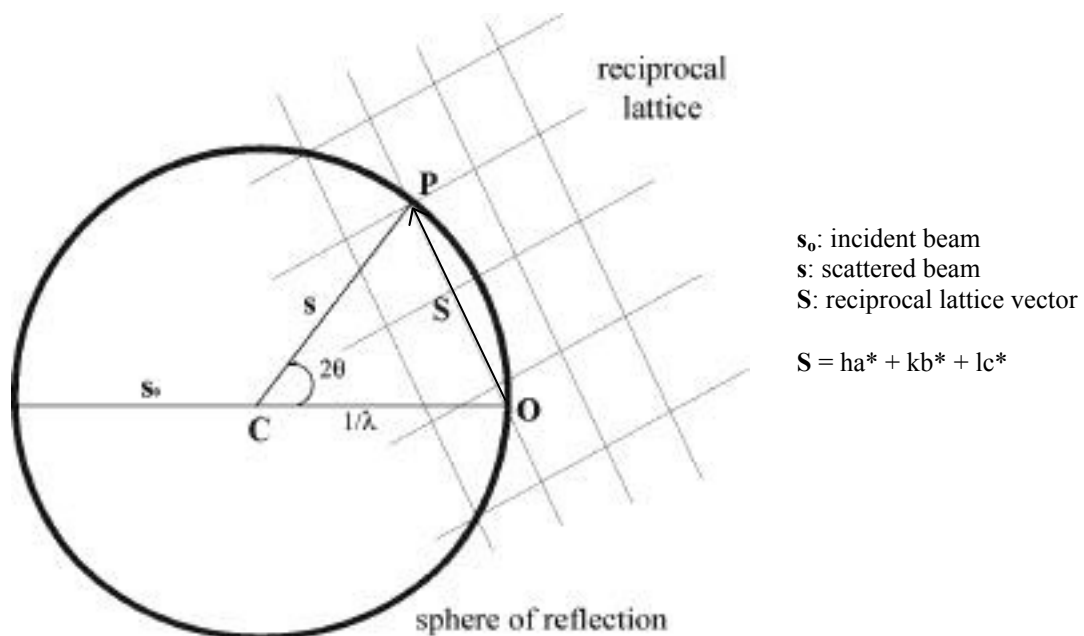**FIGURE 9.** The Ewald construction. In reciprocal space, the crystal is placed in the centre of a sphere (C) with radius 1/ . The origin of the reciprocal lattice is placed at O (i.e., reflection (0 0 0)). The reciprocal lattice will rotate as the crystal does and only the reciprocal lattice points that intersect with the Ewald sphere will be recorded (in real space) on an image plate detector.

As reciprocal lattice we understand a theoretical lattice that is useful for constructing the directions of diffraction because it rotates exactly as the crystal does. In the reciprocal lattice, the planes are perpendicular to the real space planes and the reciprocal lattice unit cell axes are a* = 1/a, b* = 1/b and c* = 1/d. A set of planes (hkl) produces the reflection hkl in the direction CP (**s**) when the reciprocal point $P_{hkl}$ contacts the sphere.

### 1.2.3. Solution of the crystal structure: searching for heavy atom derivatives

One problem, the so-called phase problem, arise after collection of X-ray diffraction data: the intensities can be directly extracted, $I(hkl)$   $|F(hkl)|^2$, from the experiment, but no phase information is available in order to obtain each $F(hkl)$ structure factor:

$$F(hkl) = |F(hkl)|\exp i \ (hkl) \qquad \textbf{(equation 2)}$$

$$\underbrace{\hspace{2cm}}_{\text{Amplitude}} \underbrace{\hspace{2cm}}_{\text{Phase angle}}$$

The electron density (_) for all points (x,y,z) in the crystal cell can only be calculated if both the amplitude and the phase are known for each (hkl) plane reflection:

$$\_(x,y,z) = (1/V) \sum_{hkl} |F(hkl)|\exp(i \ _{hkl})\exp[-2 \ i(hx + ky + lz)] \qquad \textbf{(equation 3)}$$

Several methods can be used to overcome the phase problem of protein crystallography: Molecular Replacement (MR), Single Isomorphous Replacement (SIR), Multiple Isomorphous Replacement (MIR), and Multiple-wavelength Anomalous Dispersion (MAD).

The Patterson function (Patterson, 1934) is the Fourier transform of $|F(hkl)|^2$ and it may be calculated from any set of recorded diffraction intensities:

$$P(uvw) = (2/V) \sum_{hkl} |F(hkl)|^2 \cos 2\pi (hu + kv + lw) \qquad \textbf{(equation 4)}$$

The information that can be extracted from the Patterson functions are all possible interatomic vectors. But it cannot be interpreted directly if the structural complexity exceeds a determinate limit, as in the case of a protein structure. However, under certain conditions the Patterson function allows the location of single atoms in the protein structure. As prerequisite these atoms have to have a large number of electrons (i.e., heavy atoms).

For PNP synthase, the method used to solve the phase problem was the SIR method including anomalous diffraction. That method, as well as MIR, is based on the introduction of a heavy atom as a new scatterer of high atomic number. Its presence must not disturb the crystal packing of the macromolecule because it is essential that native and derivative(s) structures are isomorphous. The way to introduce such an atom is either soaking the crystals or co-crystallising it together with the protein. The stable addition of one or more heavy atoms will introduce differences in the diffraction pattern respect to that of the native protein:

$$\mathbf{F_{PH}} = \mathbf{F_P} + \mathbf{F_H} \qquad \textbf{(equation 5)}$$

where $\mathbf{F_P}$ is the structure factor of the protein (with amplitude $F_p$ and phase $\alpha_P$). $\mathbf{F_H}$ and $\mathbf{F_{PH}}$ are the structure factors of the heavy atom and the corresponding derivative (protein + heavy atom), respectively. The position of the heavy atom can be calculated from a difference Patterson map between the derivative and the native protein and after refinement of this position(s) the protein phases can be solved (Fig. 10).
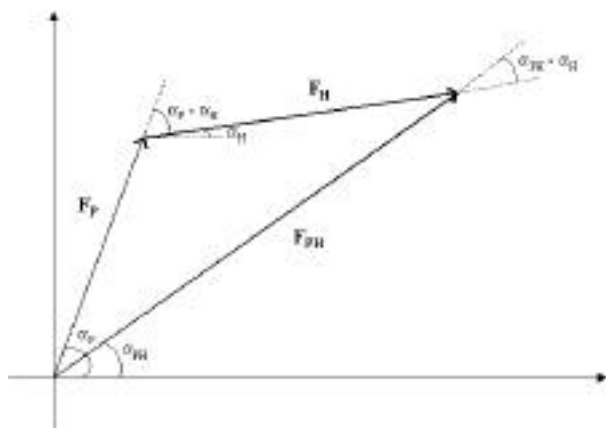
23

**FIGURE 10.** The phase problem. A vector diagram illustrating the native protein ($F_P$) and heavy atom ($F_H$) contributions to the structure factor for the heavy atom derivative of the protein ($F_{PH}$). The structure factor amplitudes and phases defined in the text are indicated.

As illustrated in the Harker diagram (Figure 11A), two solutions for $\alpha_P$ exist for each heavy atom derivative. This ambiguity can be solved if a second different scatterer is present because the correct solution will coincide in both cases (Fig. 11B). For the isomorphous replacement method, the need of several derivatives is more common than the use of a single one. Thus, in most cases a large variety of heavy atom compounds have to be screened to identify suitable isomorphous heavy atom derivative (e.g., Hg, Pt, U, Au, Ag containing sample). The finding of these derivatives is normally a non-rational approach. Heavy atom analogues of the substrate(s) or product(s), metal ion cofactors or replacement of an amino acid with a heavy atom labelled analogue may be good alternatives to use instead of soaking or co-crystallising with a heavy atom solution. Blundell and Johnson classified compounds as 'hard', that bind without covalent interactions, and 'soft', that bind covalently to sulfhydryl, imidazole and thiol groups (Blundell and Johnson, 1976). The best choice of atom type will depend on its diffraction properties rather than its chemical properties. The first criterion will be whether the total scattering is enough to be observed experimentally. In isomorphous replacement, this simply depends on the number of heavy atoms to be positioned and on their atomic number.
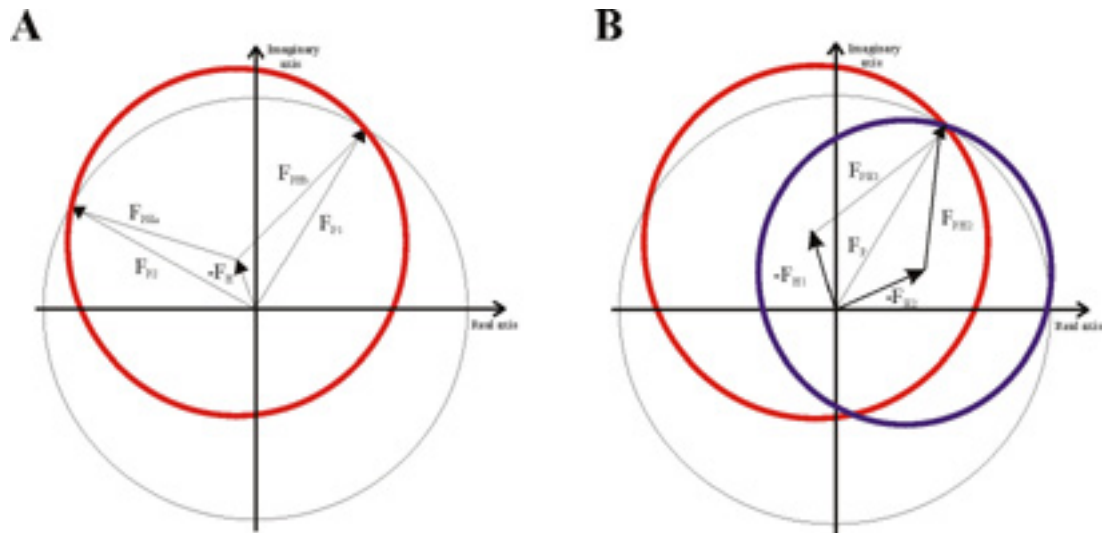
**FIGURE 11.** The Harker diagram for protein phase determination. **A)** Case where only one heavy atom is present. A circle of radius $|F_P|$ is drawn and from its center, the vector $-\mathbf{F_H}$. A second circle (in red) with $|F_{PH}|$ radius is drawn at the endpoint of $F_H$. The intersections of the two circles correspond to two equally probable protein phase angles. Both triangle fulfil the condition $\mathbf{F_{PH}} = \mathbf{F_P} + \mathbf{F_H}$ **B)** Case where two different heavy atoms are present. In this situation it is easier to elucidate which is the correct solution because the drawn circles ideally intersect at the same position.

# 2. PUBLICATIONS

**2.1. Garrido-Franco, M.**, Huber, R., Schmidt, F.S., Laber, B. and Clausen, T. (2000). Crystallization and preliminary x-ray crystallographic analysis of PdxJ, the pyridoxine 5'-phosphate synthesizing enzyme. *Acta Cryst. Sect. D* **56**:1045-1048.

**Acta Crystallographica Section D. Biological Crystallography.**

**CRYSTALLIZATION PAPERS**

# Crystallization and Preliminary X-ray Crystallographic Analysis of PdxJ, the Pyridoxine 5'-Phosphate Synthesizing Enzyme.

Marta Garrido-Franco[1], Robert Huber[1], Frank S. Schmidt[2], Bernd Laber[2] and Tim Clausen[1*]

[1] Max-Planck-Institute of Biochemistry, Department of Structural Investigation, Am Klopferspitz 18a, D-82152 Martinsried, Germany

[2] AgrEvo GmbH, Hoechst Schering, Werk Biochemie, D-65926 -Frankfurt, Germany

[*] To whom correspondence should be addressed. Email: clausen@biochem.mpg.de

**Abbreviations**

ASU, asymmetric unit; DXP, 1-deoxy-D-xylulose-5-phosphate; EMTS, ethyl mercury thiosalicylate; MPD, 2-Methyl-2,4-pentanediol; PLP, pyridoxal 5'-phosphate; PMP, pyridoxamine 5'-phosphate; PN, pyridoxine, vitamin $B_6$; PNP, pyridoxine 5'-phosphate.

**Abstract**

The enzyme PdxJ catalyzes the condensation of 1-deoxy-D-xylulose-5-phosphate (DXP) and 1-amino-3-oxo-4-(phosphohydroxy)propan-2-one to form pyridoxine 5'-phosphate (PNP). The protein from *Escherichia coli* has been crystallized in several forms under different conditions. The best diffracting crystals were obtained by a combination of the hanging drop vapor diffusion and microseeding techniques. Using an in-house image plate, the PdxJ crystals diffracted under cryo-conditions to 2.6 Å resolution. The space group has been determined as $C222_1$ with unit-cell parameters a=132.5, b=154.4, and c=131.4 Å corresponding to four monomers per asymmetric unit. In the search for heavy-atom derivatives, a mercury derivative has been interpreted. The 12 mercury sites located are related by 222 symmetry and, in combination with self rotation search analyses and gel filtration experiments, indicate the quaternary assembly of PdxJ into octamers with 422 symmetry.

## 1. INTRODUCTION

Pyridoxal 5'-phosphate (PLP), the biocatalytically active form of vitamin $B_6$ (pyridoxine, pyridoxol; PN), acts as a central coenzyme in amino-acid metabolism. Pyridoxine is converted to PNP by the kinase PdxK (Yang *et al.*, 1996). PNP, and also pyridoxamine 5'-phosphate, are then oxidized by PdxH to PLP, which in turn can be transaminated to PNP. In addition to these salvage reactions, there is a biosynthetic pathway to yield an initial substrate that can be recycled. While bacteria, plants and fungi contain the enzymatic machinery to synthesize PN and PNP (Dempsey, 1987; Hill &

Spenser, 1986; Tryfiates, 1986), mammals lack such a biosynthetic pathway and are limited to transforming vitamin $B_6$ obtained in the diet into the other five vitamers.

In *E. coli*, the products of the three genes, *pdxA, pdxJ* and *pdxH* have been reported to be responsible for PLP biosynthesis (Lam & Winkler, 1992; Notheis *et al.*, 1995; Zhao & Winkler, 1994). PdxA catalyzes the oxidation of 4-(phosphohydroxy)-L-threonine (HTP) to 1-amino-3-oxo-4-(phosphohydroxy)propan-2-one (Cane *et al.*, 1998) in a $NAD^+$-dependent reaction. The condensation and subsequent ring closure reaction of 1-deoxy-D-xylulose-5-phosphate and 1-amino-3-oxo-4-(phosphohydroxy)propan-2-one to yield PNP is carried out by PdxJ (Laber *et al.*, 1999). The PNP oxidation to PLP, the last step in the biosynthesis pathway, is catalyzed by the PdxH oxidase (Dempsey, 1980; Hill & Spenser, 1986). Recent studies of PLP biosynthesis and the established roles of PdxA and PdxJ confirm that the $B_6$ vitamers are synthesized *de novo* and are not only interconverted into each other (Dempsey, 1966; Hockney & Scott, 1979).

PdxJ consists of a single polypeptide chain of 242 amino acids (27.5 kDa) which appears to form a single domain. Cane *et al.* (1998) have reported that the enzyme is a monomer in solution. From a mechanistic point of view, PdxJ is the most interesting of the three enzymes involved in PLP biosynthesis because it catalyzes the complicated ring-closure reaction yielding PNP. Furthermore, PdxJ is a potential target for the development of new antibiotics as its occurrence is restricted to bacteria.

However, none of the *E. coli* enzymes involved in PLP biosynthesis has yet been structurally characterized and no apparent homology to any other protein has been reported for any of them. Therefore, the determination of the PdxJ crystal structure and the analysis of its active-site architecture should be extremely helpful in gaining insight

into the chemically demanding steps that take place during PNP biosynthesis. Here, we present the crystallization and preliminary X-ray diffraction data of PdxJ.

## 2. MATERIALS AND METHODS

### 2.1. General methods

The PdxJ protein from *E. coli* was cloned, overexpressed and purified as reported previously (Laber *et al.*, 1999). Briefly, the *pdxJ* gene was inserted into the vector pASK-IBA3 (IBA-Institüt für Bioanalytik GmbH, Göttingen), resulting in the construct pPDXJ1. This plasmid has a C-terminal Strep-tag II (Schmidt *et al.*, 1996) affinity peptide. The gene was expressed in the *E. coli* JM83 strain in Luria-Bertani (LB) medium containing 100 µg ml$^{-1}$ ampicillin. Purification on an affinity Strep Tactin column (IBA) yielded approximately 20 mg protein per liter of cell culture.

### 2.2. Crystallization

The Hampton Research Crystal Screens I and II and our in-house factorial solutions were used to carry out initial crystallization trials. For this purpose, purified PdxJ (6 mg ml$^{-1}$ in 2mM Tris-HCl pH 8.0) was mixed and equilibrated against a 500 µl reservoir in a sitting-drop vapor-diffusion setup in a 2:1 ratio (3 µl protein solution and 1.5 µl crystallization solution). Two conditions at 293 K yielded diffracting crystals with well defined morphologies, reported here as different classes.

**2.2.1. Class I.** Triangular-shaped crystals were obtained using 0.1 M sodium acetate pH 4.6, 8% PEG 4000 as the precipitant and 0.1 M L-cysteine as an additive. Crystals appeared after 10 d (Fig. 1a).

**2.2.2. Class II.** Well diffracting rod-shaped crystals were grown using 10% PEG 6000 and 2 M NaCl as reservoir solution (Fig. 1b). Unfortunately, two problems were encountered: (i) slow crystals growth that took around six weeks and (ii) reproducibility of the crystals. Even intensive screening of crystallization parameters such as temperature, ratio of protein and reservoir, pH, protein and precipitant concentration and additives did not improve the reproducibility or the rate of crystal growth.

Crystallization could be improved by using the microseeding technique. For this purpose, small crystals were crushed into small fragments. Using a rabbit hair, seeds were placed into fresh drops consisting of an equal volume of precipitant and more concentrated protein solution (13.5 mg ml$^{-1}$ in 2mM Tris-HCl pH 8.0) and were equilibrated for 1 d. Different crystallization setups were tried, but only the hanging drop-method yielded suitable crystals. Large single crystals with a new morphology started to grow after 1 d and reached their maximum size after one week.



(a)        (b)

**Figure 1.** (a) Class I and (b) class II crystals of the PdxJ enzyme.

## 2.3. Data collection

**2.3.1. Class I.** The diffraction quality of this crystal form allowed us to collect a complete data set of 90 frames (1° oscillation range, 1500 s exposure time) to a resolution of 4.5 Å. A single crystal was mounted in a siliconized thin-wall glass capillary. For all the experiments reported here the data was collected with our in-house MAR Research (Hamburg, Germany) image-plate system mounted on a Rigaku (Tokyo, Japan) rotating-anode generator operating at 50 kV and 100 mA (Cu K_ radiation,   = 1.5418 Å). After several hours of exposure, the diffraction power of the crystal had decreased from 3.3 Å to 5.0 Å resolution (Table 1).

| | Class I | Class II | |
| | | native | thiomersal |
|---|---|---|---|
| Space group | P2 | $C222_1$ | $C222_1$ |
| Unit cell dimensions (Å) | a=87.7, b=184.6, c=146.0, ß=104.0° | a=132.5, b=154.4, c=131.4 | a=131.4, b=155.1, c=130.1 |
| Diffraction limit (Å) | 3.3 | 2.6 | 2.6 |
| Mosaicity (°) | 0.6 | 0.3 | 0.4 |

**Table 1.** Crystal characteristics.

**2.3.2 Class II.** Preliminary X-ray diffraction studies at room temperature showed that this crystal class belongs to a different space group. Initially, the resolution was 3.0 Å but, as was the case with class I crystals, it decreases rapidly upon X-ray exposure. As an attempt to avoid excessive radiation damage, a cryocooling condition was established. A cryobuffer consisting of the same precipitant supplemented with 10%(v/v) 2-Methyl-2,4-pentanediol (MPD) turned out to be suitable. Crystals were soaked for 10 s in the cryobuffer and were frozen in a nitrogen stream at 100 K (Oxford Cryosystems

Cryostream). Under these conditions, a complete data set to 2.6 Å resolution was collected using 1° oscillation range with an exposure time of 1200 s. Crystals of this class were used for further soaking attempts and heavy-atom search.

Indexing and integration of diffraction data from both crystal forms was performed using DENZO (Otwinowski & Minor, 1997). The data were scaled and merged using the SCALA program (Evans, 1991) and were placed on an absolute scale with TRUNCATE (French & Wilson, 1978).

### 2.4. Soaking with PLP

Owing the similarity of PLP to PNP, the product of the PdxJ-catalyzed reaction, PLP probably acts as a feedback inhibitor of its own synthesis. In order to determine whether PLP binds to PdxJ, crystals were soaked in solutions of different PLP concentrations (at 293 K, in the dark). After 2 h, crystals soaked at 1-10 mM PLP acquired a yellow color. Crystals in 10 mM PLP started to develop cracks, while crystals in 1 mM seemed to be unaffected. However, all PLP-treated crystals (2 h soaking and a few seconds backsoaking in cryobuffer) completely lost their diffraction power. Even with synchrotron radiation (beamline BW6, DESY, Hamburg) no reflections could be observed. The crystal cracking and associated loss of crystal order indicated that PLP is inducing spatial rearrangements of the PdxJ which are not tolerated by the class II crystal form. Further co-crystallization experiments are under way.

## 2.5. Heavy-atom derivatives

One heavy-atom derivative has been interpreted successfully. After soaking native protein crystals in 20 µl of an appropriately buffered solution containing 1 mM thiomersal (ethyl mercury thiosalicylate; EMTS, $C_9H_9HgO_2SNa$) for one week, we collected a complete derivative data set to 2.6 Å resolution.

## 2.6. Gel filtration

In order to estimate the oligomeric state of PdxJ in solution, 6 µl of sample as loaded on a Superose12 SMART column (Pharmacia) equilibrated with 100 mM Tris-HCl pH 8.0 at room temperature. As a control for the size of the separated peaks, four proteins were used to calibrate the column under the same pH and temperature conditions. These markers (Boehringer-Mannheim) were albumin (45 and 68 kDa), aldolase (158 kDa) and katalase (240 kDa), which covered the range expected for monomers to octamers of PdxJ.

## 3. RESULTS AND DISCUSSION

The space group for class I crystals was found to be P2, with unit-cell parameters a=87.7, b=184.6, c=146.0 Å, ß=104.0°. The class II crystals belongs to the orthorhombic space group $C222_1$, with unit-cell parameters a=134.5, b=154.6, c=133.4 Å at 293 K. The cryocooled crystals have contracted unit-cell parameters: a=132.5, b=154.4, c=131.4 Å. Thiomersal-soaked crystals were indexed with the same space group and unit-cell parameters: a=131.4, b=155.1, c=130.1 Å, and are isomorphous to the natives (Table 1; Fig. 1). Data-collection statistics are summarized in Table 2.

|  | Class II, native | Class II, thiomersal |
|---|---|---|
| Temperature (K) | 100 | 100 |
| Resolution range (Å) | 25.0 – 2.6 | 25.0 – 2.6 |
| Observed reflections [I > 0_(I)] | 307023 | 194829 |
| Unique reflections [I > 0_(I)] | 40732 | 40605 |
| Completeness (%) |  |  |
| Overall | 97.3 | 95.4 |
| Outer shell§ | 97.3 | 95.4 |
| I/_(I) |  |  |
| Overall | 8.2 | 5.6 |
| Outer shell§ | 3.7 | 2.0 |
| $R_{sym}$*(%) |  |  |
| Overall | 8.4 | 12.1 |
| Outer shell§ | 19.2 | 32.4 |
| Multiplicity |  |  |
| Overall | 4.5 | 2.8 |
| Outer shell§ | 4.1 | 2.3 |

*§ Outer-shell data is in the resolution range: 2.73 – 2.60*

* $R_{sym} = \_| I - (I) | / \_ (I)$

**Table 2.** Data-collection statistics.

The data from the native and the possible derivative were merged using CAD and scaled with SCALEIT (Collaborative Computational Project Number 4, 1994). SOLVE (Terwilliger & Berendzen, 1999) was used to find and refine eight heavy-atom positions. Afterwards, four new sites were found using the program SHARP (La Fortelle *et al.*, 1997) and all 12 positions, related by a 222 symmetry, were refined. The phases were then calculated, resulting in an overall phasing power of 1.9 and figure of merit of 0.36 for the whole resolution range (20.0-2.6 Å).

Based either on four (or five) molecules per asymmetric unit (ASU), the solvent content is calculated to be 49% (36%), corresponding to a Matthews coefficient $V_M$ of 2.39 $\text{Å}^3\,\text{Da}^{-1}$ (1.91 $\text{Å}^3\,\text{Da}^{-1}$) for class I (Matthews, 1968). Assuming four molecules per ASU ($V_M = 2.77\ \text{Å}^3\,\text{Da}^{-1}$), class II crystals contain approximately 56% solvent.

Self-rotation functions were calculated on the scaled data from class II native crystals (Fig. 2) using the program GLRF (Tong & Rossmann, 1997). In the _ = 180° section (Fig. 2a), in addition to the peaks corresponding to the crystallographic twofold axis, a local dyad in direction of the *ac* diagonal is obvious. The _ = 90° section (Fig. 2b) presents a strong peak arising from a local fourfold axis parallel to *b*. Assuming four PdxJ molecules per ASU, these calculations, together with the 222 symmetry deduced from the heavy-atom positions, suggest a 422 symmetric octamer of PdxJ. It had been previously reported by Cane *et al.* (1998) that PdxJ is active as a monomer. In order to confirm our suggestion that PdxJ is an octamer in solution, we performed a gel filtration experiment (Superose12, Pharmacia). In several runs, PdxJ eluted between $K_{av}$ values of 0.630 and 0.638 corresponding to a molecular mass of 240 ± 10 kDa (Fig. 3). With the molecular weight of 27.5 kDa calculated from its sequence, the gel filtration confirms that PdxJ is an octamer.

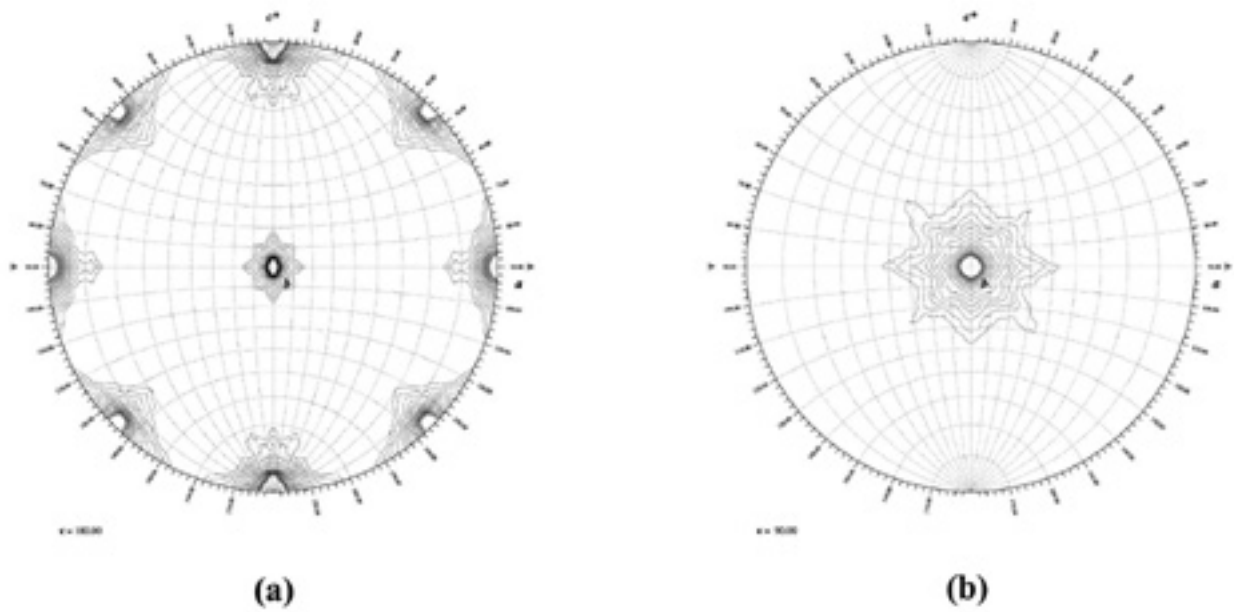(a)                                                (b)

**Figure 2.** Stereographic projection of the self-rotation function in spherical polar angles. Diffraction data in the resolution range 15.0-2.6 Å were used, with a Patterson integration radii of 30 Å. (a)    = 180°, with a peak high of 23.8 and 12.5    for the crystallographic and non-crystallographic dyad axes, respectively. (b) = 90°, with a maximum peak height of 15.7  .
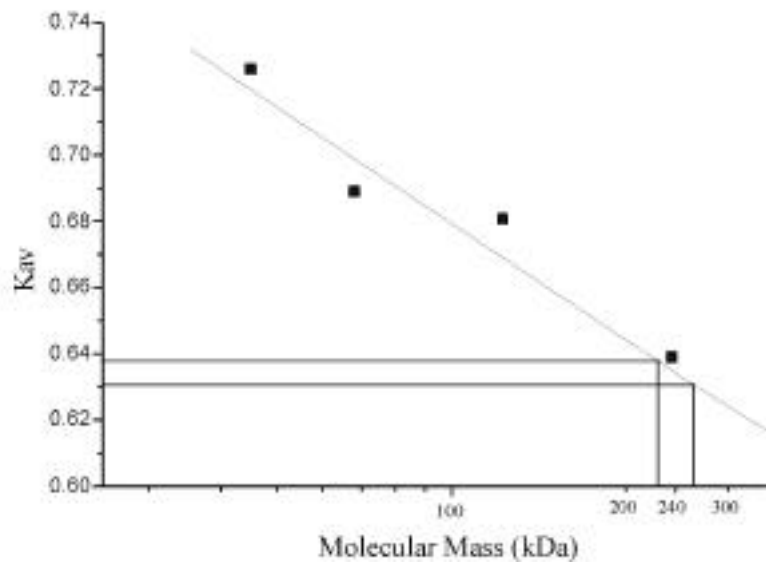


**Figure 3.** Native molecular mass estimation of PdxJ as performed by gel filtration (Superose12, Pharmacia).

## REFERENCES

Cane, D. E., Hsiung, Y. J., Cornish, J. A., Robinson, J. K. & Spenser, I. D. (1998). *J. Am. Chem. Soc.* **120**, 1936-1937.

Collaborative Computing Project Number 4 (1994). *Acta Cryst. Sect. D* **50**, 760-763.

Dempsey, W. B. (1966). *J. Bacteriol.* **92**, 333-337.

Dempsey, W. B. (1980). *Biosynthesis of control of Vitamin B₆ in Escherichia coli*, edited by G. P. Tryfiates, pp. 93-111- Westport, Connecticut: Food and Nutrition Press.

Dempsey, W. B. (1987). Escherichia coli and Salmonella typhimurium: Cellular and Molecular Biology, edited by F. C. Neidhardt, J. L. Ingraham, K. B. Low, B. Magasanik, M. Schaechter & H. E. Umbarger, pp. 539-543. Washington, DC: American Society for Microbiology.

Evans, P. R. (1991). Crystallographic Computing 5, edited by D. Moras, A. D. Podjarni & J. C. Thierry, pp. 136-144. Oxford University Press.

French, S. & Wilson, K. (1978). Acta Cryst. Sect. A **34**, 517-525.

Hill, R. E. & Spenser, I. D. (1986). *Vitamin B₆ Pyridoxal Phosphate*, Part A, Vol. 1, edited by D. Dolphin, R. Poulson & O. Avramovic, pp. 417-476. New York: Wiley Interscience.

Hockney, R. C. & Scott, T. A. (1979). *J. General Microbiol.* **110**, 275-283.

La Fortelle, E. D., Irwin, J. J. & Bricogne, G. (1997). *Crystallogr. Comput. 7*, edited by P. E. Bourne & K. D. Watenpaugh, pp. 1-9. Oxford University Press.

Laber, B., Maurer, W., Scharf, S., Stepusin, K. & Schmidt, F. S. (1999). *FEBS Lett.* **449**, 45-48.

Lam, H.-M. & Winkler, M. E. (1992). *J. Bacteriol.* **174**, 6033-6045.

Matthews, B. W. (1968). *J. Mol. Biol.* **33**, 491-497.

Notheis, C., Drewke, C. and Leistner, E. (1995). *Biochim. Biophys. Acta* **1247**, 265-271.

Otwinowski, Z. & Minor, W. (1997). *Methods Enzymol.* **276**, 307-326,

Schmidt, T. G. M., Koepke, J., Frank, R. & Skerra, A. (1996). J. Mol. Biol. **255**, 753-766.

Terwilliger, T. C. & Berendzen, J. (1999). *Acta Cryst. Sect. D* **55**, 849-861.

Tryfiates, G. P. (1986). *Vitamin B₆ Pyridoxal Phosphate*, Part B, edited by D. Dolphin, R. Poulson & O. Avramovic. New York: Wiley Interscience.

Tong, L. & Rossmann, M. G. (1997). *Methods Enzymol.* **276**, 594-611,

Yang, Y., Zhao, G. S. & Winkler, M. E. (1996). *FEMS Microbiol. Lett.* **141**, 89-95.

Zhao, G. & Winkler, M. E. (1994). *J. Bacteriol.* **177**, 883-891.